Journal of Computers Vol. 34 No. 5, October 2023, pp. 1-14
doi: 10.53106/199115992023103405001

Reconstruction of Communication Signal in Wireless Networks Based on Perturbation Compression Perception

Juan Wang*

School of Network and Communication, Nanjing Vocational College of Information Technology, Nanjing, 210023, China

zhoucl2016@163.com

Received 22 August 2022; Revised 30 December 2022; Accepted 10 February 2023

Abstract. With the maturity and development of new generation communication technology, the demand for wireless network communication quality is getting higher and higher. However, the existing wireless network data transmission models are greatly affected by the signal quality in the data transmission process, which seriously affects the quality of data transmission. To address the problem of signal perturbation affecting communication quality in wireless network communication, this study designs an improved perturbation compression reconstruction algorithm that can be used to process block-structured data based on the block sparse structure in the original signal, and constructs a single-user wireless network communication data transmission model based on this algorithm. The performance simulation test of the model shows that the MSE values of the model are lower than those of the conventional and perfect schemes used as comparisons under the same noise conditions and the transmitted compressed data length conditions. When the variance of Gaussian white noise is 0.125, the MSEs of the research design model, the conventional scheme and the perfect scheme are 0.031, 0.048, and 0.047, respectively. Experimental data show that the improved disturbance compressed sensing reconstruction algorithm can better reconstruct the compressed information and reduce the information loss caused by the disturbance in the compression process on the premise of removing the signal disturbance. This research result has reference significance for improving the signal quality of wireless network communication.

Keywords: perturbation compression-aware reconstruction, wireless networks, communication signals, block sparse structure, channel

1 Introduction

At present, the world is in the age of big data. Faced with a large amount of data information, people need to timely collect, screen and effectively transmit data from them. Traditional data sampling methods limits the communication efficiency to some extent as demonstrated [1]. To meet the requirements of big data applications in the aspect of accuracy, traditional communication systems are often overloaded, which can increase the system operation cost significantly, although the development of modern data compression technology has alleviated this problem to some extent as demonstrated [2]. However, the existing methods of communication signal acquisition and transmission lead to a more serious signal perturbation problem, which has the most significant impact on wireless communication networks in reference [3]. To reduce the negative impact of signal perturbation on wireless communication systems, it is of great value to explore better methods for processing and transmitting communication signals as demonstrated [4]. Compressed sensing is an information guidance theory that breaks away from traditional sampling methods. It is often used in communication signal construction to achieve relatively good reconstruction of perturbed information in reference [5]. Therefore, this research innovatively applies the emerging compression sensing technology to wireless data transmission, and reconstructs the wireless network communication signal to synchronously ensure the realization of communication signal and communication efficiency. This research improves the perturbation compression-aware reconstruction algorithm used for wireless communication information processing and designs a theoretically feasible single-user transmission model for wireless network communication signals based on the improved algorithm. Simulation experiments are also designed and conducted to verify the performance difference between the designed wireless network communication signal transmission model and other common traditional models.

* Corresponding Author

This paper has done some research work in improving the quality and efficiency of data transmission, and has made some research achievements. The compressed sensing reconstruction algorithm is used to optimize the data transmission model. The optimized model is more efficient and accurate in data transmission. It is superior to the traditional data transmission model. This research result can effectively meet the demand for data quality in the process of large-scale data transmission.

The research content mainly includes four parts. The first part is the introduction. The second part summarizes the research status of compression sensing technology and communication signal network design at home and abroad. The third part introduces the application research of improved compression sensing reconstruction algorithm in wireless communication network. An improved data disturbance sensing reconstruction algorithm for wireless communication network is designed in section 1. In section 2, a wireless communication network data transmission model based on disturbance compression sensing is constructed. In the fourth part, the proposed method is tested and analyzed, and the performance of the data disturbance compressed sensing reconstruction algorithm and the improved wireless data transmission model are introduced respectively. The results show that the proposed wireless network communication signal reconstruction method based on disturbance compressed sensing has good data transmission effect.

2 Related Works

In recent years, more and more people have started to study the application value of compressed sensing theory in the field of information processing. Cao et al. proposed a method for power quality disturbance signal identification by extracting features from compressed sensing sparse vectors. The method was based on compressed sensing theory, and the new measurement signal was obtained by sampling the original signal and using orthogonal matching tracking algorithm to obtain sparse vectors for simulation experiments, the results showed that the method had a substantial increase in the number of features extracted than the original method, and the average accuracy of the method was up to 98.71% as demonstrated [6]. Wang et al. proposed a set of signal acquisition methods for power quality disturbance signals, and applied the acquisition method to data compression. The results showed that the method can effectively reduce the memory requirement of the acquisition device and improve the transmission rate in reference [7]. Liu and Tang [8] proposed a generalized correlation calculation step of the matrix by deriving the orthogonality and non-singularity of the matrix. On this basis, they also conducted experiments on the compression and reconstruction of the power quality disturbance signal. The results showed that the calculation model had obvious non-coherence. Saeed et al. used MQTT as a network protocol and deployed different sensor nodes to collect data from the environment to propose a smart city construction architecture, which was realized by using a lightweight and easy to implement network design and a simpler data format for information exchange in reference [9].

With the rapid development of wireless network technology, how to ensure the stability of wireless network communication signals under different coverage areas has become an urgent problem in the field of wireless technology. Jiang et al. [10] designed a network ideology big data platform for the hazard of ideology infiltration into the network, and analyzed the detection capability and running time of the platform. The results showed that the performance of the network data platform was better than the previous network model, with better ability to capture signals to prevent ideology infiltration into the network. Shi et al. [11] proposed a power coverage area for a typical outdoor scenario to evaluate the power coverage of wireless communication by adjusting the RIS to obtain more coverage areas. Due to the high computational complexity of the optimal solution, the calculation method was optimized and the results showed that the power coverage could be improved. Wang et al. [12] used deep CNN to learn time domain signal features of different lengths to improve the modulation of traditional methods for fast and accurate signal identification, and also to solve the limitation of fixed length of input data in traditional DLM. The experiments showed that the recognition effect under this network better than the traditional network. The training time of this network was also shorter than that of the traditional network. Naman et al. [13] designed a new control system that set up authentication through wireless network and displayed web pages to the user immediately after connecting to the radio signal and automatically obtaining the IP address, thus solving the wireless network. The performance of the system was tested. It was found that the system enabled authorized users to obtain authentication and maximize the use of network resources.

It can be seen from the above that the research on compression sensing technology and communication signal network design is relatively rich, but most of the existing network communication transmission technologies cannot give consideration to both signal quality and communication efficiency. Therefore, the research combines the

advantages of the compression sensing technology and innovatively applies the disturbance compression sensing technology to reconstruct the wireless network communication signals. Constructing a wireless communication network data transmission model based on the disturbance compression sensing is an effective way to meet the actual requirements of communication signals and communication efficiency.

3 Research on the Application of Modified Machine Perturbation Compression-aware Reconstruction Algorithm in Wireless Communication Networks

3.1 Improved Data Perturbation-aware Reconstruction Algorithm Design for Wireless Communication Networks

The traditional perturbation compressive-aware reconstruction algorithm has the problem of insufficient reconstruction accuracy, while in the compressive-aware reconstruction algorithm, the block sparse structure in the original signal is used to enhance the reconstruction accuracy of the data. This approach can also be transferred to the solution of the perturbation compressive-aware reconstruction problem [13]. However, the current traditional perturbation compression perceptual reconstruction algorithm does not consider this approach to enhance the quality of information reconstruction [14]. Therefore, this study attempts to design an improved perturbation-compression-aware reconstruction algorithm that can be used for block-structured data of the original data [15]. The algorithm contains a block-structure-based perturbation correction mechanism that enables block-by-block correction of the support set, thus reducing the reconstruction errors caused by perturbations [16]. A detailed analysis of the improved data perturbation compressed-aware reconstruction algorithm for wireless communication networks is presented below. Under perturbation state, the signal in the compressed-aware sampling model expresses sparsity through Eq. (1).

$$\hat{A} = A + E \cdot \tag{1}$$

E, A, and $\hat{A}$ are the i-unknown perturbation matrix of information, the measurement matrix and the measurement matrix of superimposed sparsity respectively. Due to the sparsity of wireless network data, information compression perception reconstruction will be significantly disturbed, so it can be assumed that the intensity of the perturbed objects is substantially smaller than the known objects in A. The problem of compression perception reconstruction in the presence of perturbation can be described through Eq. (2).

$$\min \left\| X \right\|_0 \ s.t. \ \min_{E \in \Delta} \left\| y - (A + E)x \right\|_2 < \varepsilon \ . \tag{2}$$

In Eq. (1), Δ represents the constraint on the perturbation. X is the input block sparse signal. $\|\cdot\|_n$ represents the first parametric. n y is the corresponding measurement of the block sparse signal. ε is the upper limit of the noise amplitude. Eq. (2) is essentially a class of combinatorial optimization problems, which are commonly solved by the L_1 parametric relaxation method, but the reconstruction accuracy and computational complexity of this solution method are poor. Therefore, the greedy algorithms are adopted to solve the problem so as to reduce its complexity. In the first iteration of these greedy reconstruction algorithms k, the perturbed measurements y can be split into $y_{//}$ and $y_{\perp}$ by the matrix A, which represent the projection of the measurements in the corresponding submatrix space of the support set and the corresponding orthogonal residuals respectively. To maximize $y_{//}$, it is necessary to cut $y_{\perp}$. The block sparse structure in the original signal can also be expressed using Eq. (3).

$$y = \sum_{i=1}^{i=k} A[i]x[k] + y_{\perp} \ . \tag{3}$$

So after cutting the method of $y_{\perp}$ and expanding it to block sparse condition, the Eq. (4) can be obtained.

$$\hat{A}[i] = A[i]\cos(\theta_i) + \frac{y_{\perp} x^T[i]}{\left\| y_{\perp} \right\|_2 \left\| x[i] \right\|_2} \sin(\theta_i) \ . \tag{4}$$

$\hat{A}[i]$, $A[i]$ are the corrected column dictionary vector and the corrected column dictionary vector respectively, and θ_i is the rotation angle of the corresponding support set. When the perturbation correction is allowed to be large, the corrected measurement matrix projection components can be aligned with the measurement components themselves, as shown in Fig. 1.

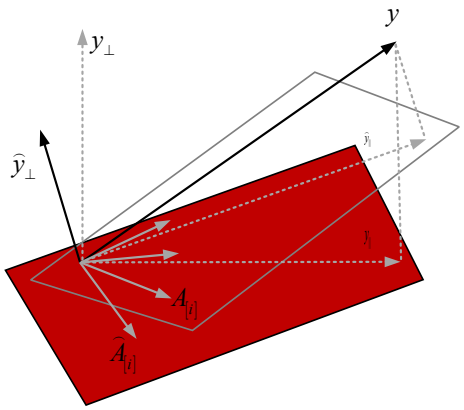

Fig. 1. Schematic diagram of the spatial correction of the measurement matrix

From Fig. 1, the constraints used to correct θ_i are the same as the perturbation space limits in essence, so the constraint settings are determined by the perturbation space limits. The following is an example of a simple constraint to illustrate the process of determining the constraints, as shown in Fig. 2.

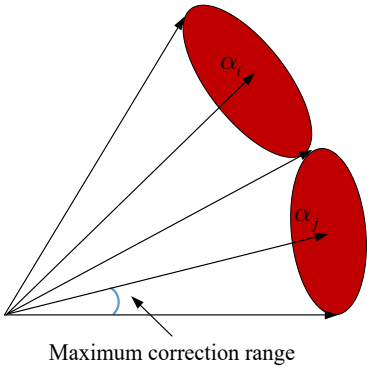

Fig. 2. Schematic diagram of the over-correction phenomenon of the measurement matrix

Observing Fig. 2, it can be seen that to satisfy the extreme values of the perturbations of each vector in each calculation do not lead to overlapping perturbations of the cones around the column information, the maximum value of the parameter θ_i should be restricted to be less than 0.5 times the minimum angle between the blocks of information, i.e. $\cos(2\theta_{\max}) \le \mu_B(A)$. μ_B is the correlation coefficient between the blocks of information [17]. The equation (4) can eliminate the influence of perturbations on the reconstruction process. But before that, it is necessary to find the parameter θ that meets the requirements of the calculation, for which further analysis of the correction mechanism is required. When the communication information satisfies $\sum_{i=1}^{i=k} \|x[i]\|_2 \tan(\theta_i) \le \|y_\perp\|_2$, the upper bound of $\|\hat{y}_\perp\|_2$ can be expressed in Eq. (5).

$$\left\|\hat{y}_{\perp}\right\|_2 \le \left\|y_{\perp}\right\|_2 \left(1 - \frac{\sum_{i=1}^{k} \left\|x[i]\right\|_2 \tan(\theta_i)}{\left\|y_{\perp}\right\|_2} \right). \tag{5}$$

The proof of equation (5) is given below, and equation (6) is obtained by comparing Eq. (3) and Eq. (4).

$$y = y_{\perp} \left(1 - \sum_{i=1}^{k} \frac{\left\|x[i]\right\|_2}{\left\|y_{\perp}\right\|_2} \tan(\theta_i) \right) + \sum_{i=1}^{k} \hat{A}[i] \sec(\theta_i) x[i] . \tag{6}$$

Considering the spherical orthogonal projection of the communication message with the parametric number of $L_2P\perp(X, y)$ is not greater than 1 and $\sum_{i=1}^{i=k} \left\|x[i]\right\|_2 \tan(\theta_i) \le \left\|y_{\perp}\right\|_2$, Eq. (6) combined with Eq. (5) can be calculated. And it can also be deduced that when the communication message satisfies the condition of Eq. (7).

$$\sum_{i=1}^{i=k} \left\|x[i]\right\|_2 \tan(\theta_i) \le \left\|y_{\perp}\right\|_2 . \tag{7}$$

The upper bound of $\left\|\hat{y}_{\perp}\right\|_2$ in Eq. (5) will show a monotonically decreasing law with the growth of the parameter θ_i , and the inference process will not be repeated this time. This leads to Corollary 1 and Theorem 1. Corollary 1 is that if the perturbation parameters satisfy $\theta^* = \tan^{-1}\left(\left\|y_{\perp}\right\|_2 / \left\|x\right\|_{2,1}\right)$, $\theta_i = \theta^* (1 \le i \le k)$, then $\left\|\hat{y}_{\perp}\right\|_2 = 0$, and the sparse signal $\left\|\hat{y}_{\perp}\right\|_2 < \varepsilon$ obtained from the reconstruction also has zero corresponding residuals. Theorem 1 is that if the parameters used for the correction satisfy $\theta_i = \theta^* = \tan^{-1}\left(\left\|y_{\perp}\right\|_2 - \varepsilon / \left\|x\right\|_{2,1}\right)$, the corresponding residuals of the measurement matrix after the correction process satisfy $\left\|\hat{y}_{\perp}\right\|_2 < \varepsilon$.

The above analysis provides a means to reduce the influence of communication information perturbations on the reconstruction process. Specifically, the treatment can be expressed as follows: when there is no noise, the method specified in Corollary 1 can be used to calculate θ^* combined with equation (4) to correct the measurement matrix in order to eliminate the perturbation influence. If data noise is present, the method specified in Theorem 1 should be used to calculate θ^*, thus eliminating the perturbation effects. It can be seen that only the corresponding additions to the existing compression-aware reconstruction algorithm are needed to obtain a compression-aware reconstruction algorithm that can eliminate or reduce data perturbations. The improved algorithm will be described in the subsequent contents. The improved compression-aware reconstruction algorithm for block structure under perturbation is based on the Block Orthogonal Matching Pursuit (BOMP for short) algorithm. However, the addition of correction parameters and corresponding steps to the BOMP algorithm downgrade the accuracy of reconstructing the original information, although it reduces both the effect of perturbation. When the BOMP algorithm reconstructs the information at a very large angle, the algorithm may stop running at the risk of having insufficient sparsity. Therefore, a restriction should be added to the corrected angle parameter of the perturbation θ to identify and exclude this operation. The added restriction is shown in Eq. (8).

$$\theta = \min(\theta^{\circ}, \theta^*) . \tag{8}$$

θ^* is the parameter obtained by Theorem 1 and θ° is the parameter attained by user-defined. According to Eq. (8), θ° should use 0.5 times the maximum angle of each block less than A as the value to prevent the column information in the dictionary from being modified by misalignment. It can be seen that the parameter θ^* needs to be small enough for the algorithm to control the residuals below the termination condition, thus ensuring the quality of the information reconstructed by the algorithm. The improved BOMP algorithm is called PBOMP, and its computational flow is shown in Fig. 3.

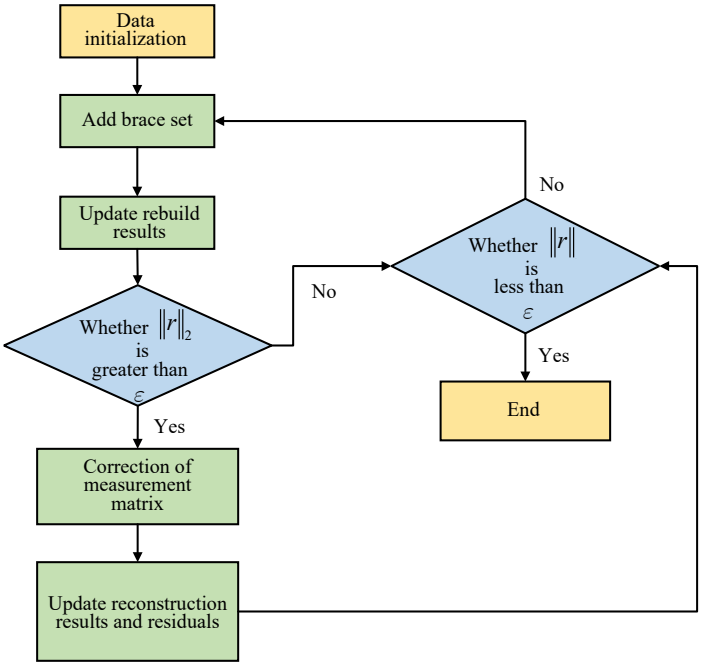

Fig. 3. Flow chart of PBOMP calculation

As shown in Fig. 3, unlike the BOMP algorithm, the PBOMP algorithm corrects the matrix task corresponding to the support set by orthogonal residuals r. The parameters required in the correction process θ are derived by Theorem 1 and are constrained by Equation (8) to ensure the accuracy of the communication information reconstruction results. Moreover, when the correction of the measurement matrix is completed, the PBOMP algorithm will calculate the residuals by updating them with the newly generated $\hat{A}$. This process will be cycled several times until the algorithm reaches the stopping condition.

3.2 Construction of Data Transmission Model for Wireless Communication Networks based on Perturbation Compression Awareness

The wireless communication network data transmission model is now constructed on the basis of the designed improved perturbation compression-aware algorithm [18]. Specifically, in the traditional wireless communication data transmission method, compressive sensing can ensure that the model as a whole completes compressive sampling of data at a lower cost, but compressive sensing also affects the sensitive characteristics of the measurement matrix. It reduces the data reconstruction accuracy and leads to its limited application prospects [19]. In addition, the data transmission frame structure in wireless communication networks is shown in Fig. 4.

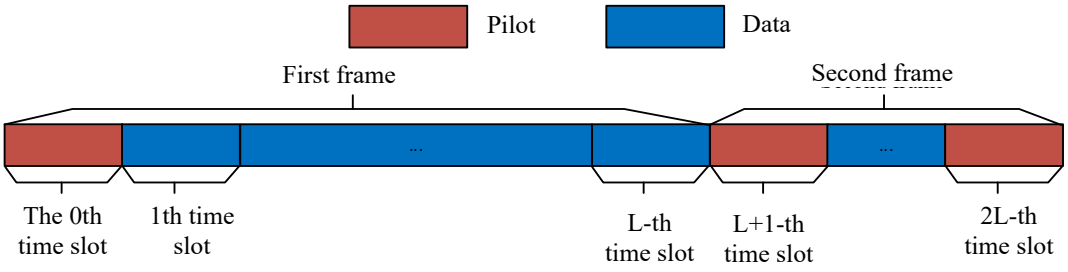

Fig. 4. Transmission frame structure of data in wireless communication network

In order to solve the contradictory problem of data reconstruction accuracy and transmission efficiency in the data transmission model of wireless communication network, a data transmission model of wireless communication network based on improved perturbation compression sensing algorithm are proposed. The overall computational flow of this model is shown in Fig. 5.

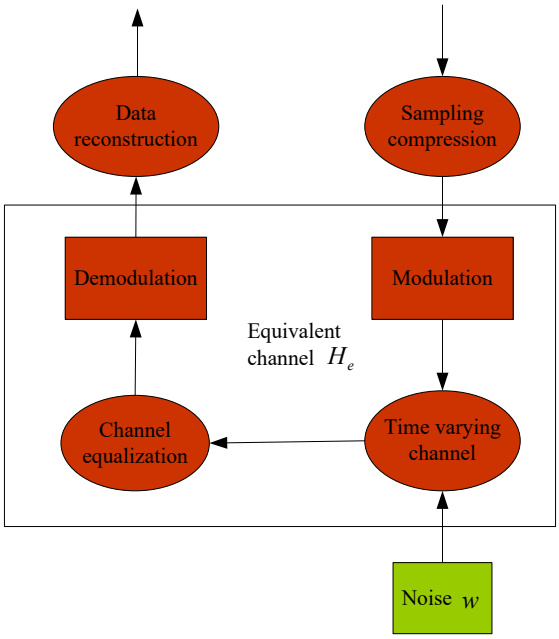

Fig. 5. Computational flow of data transmission model of wireless communication network based on improved perturbation compression-aware algorithm

The design process of the model is described in detail below. Firstly, the compressed data transmission model needs to be optimally designed in conjunction with the perturbation compression sensing principle, so that the new model can be better applied in the slow time-varying channel wireless channel scenario. The data of the l time slot is reconstructed as shown in Eq. (9).

$$\min \left\| x^{(l)} \right\|_1 \ s.t. \left\| y^{(l)} - H_e^{(l)} A x^{(l)} \right\|_2 < \varepsilon \,. \tag{9}$$

In Eq. (9), $H_e^{(l)} = \hat{H}^{(l)-1} - H^{(l)}$ represents the equivalent channel matrix of the l time slot. $H^{(l)}$ is the channel matrix of the current period, $H^{(l-1)}$ is the channel matrix of the previous period, and the relationship between them is shown in Eq. (10).

$$H^{(l)} = H^{(l-1)} + \Delta H^{(l)} \,. \tag{10}$$

In Eq. (10), $\Delta H^{(l)}$ is used to describe the variation of this channel matrix. If the true channel estimate of the $l-1$ time slot is $H^{(l-1)}$, consider it as the channel estimate of the l time slot, which is $H_e^{(l)} = I + H^{(l-1)^{-1}} \Delta H$, and thus to obtain the equivalent channel matrix of the l time slot, as shown in Eq. (11).

$$H_e^{(l)} = I + H^{(l-1)^{-1}} \Delta H^{(l)} 0 \,. \tag{11}$$

In real situation, the channel value is generally estimated only for time slot 0, the equivalent channel matrix for time slot l can be expressed as: $H_e^{(l)} = I + \sum_{i=1}^{l} H^{(0)-1}\Delta H^{(i)}$. From this, Eq. (9) can be optimized to obtain Eq. (12).

$$\min\left\|x^{(l)}\right\|_1 \ s.t.\left\|y^{(l)} - \left(A + E^{(l)}\right)x^{(l)}\right\|_2 < \varepsilon . \tag{12}$$

In Eq. (12), $E^{(l)} = \sum_{i=1}^{l} H^{(0)-1}\Delta H^{(i)}A$, where the matrix A is the known condition and the matrix $E^{(l)}$is the unknown condition. In view of the low rate of change of the channel, the change in the value of $\Delta H^{(l)}$ between two similar channels $H^{(l)}$ and $H^{(l-1)}$ is also small. It can be seen that when the value of l is small, $E^{(l)}$ is significantly lower than the value of the elements in A, which meets the condition of perturbation compression perception. Therefore, the model estimates the channels with closer spaced time slots, and the error values obtained are also smaller. The reconstruction operation of the original data can be done accurately in combination with the perturbation-compression-aware reconstruction algorithm [20]. Meanwhile, when the distance between two time gaps 0 and l is larger, the gap between the matrices corresponding to the two time gaps, i.e., the unit matrix and $H_e^{(l)}$, is also larger. The larger the perturbation strength is, the worse the performance of the perturbation reconstruction algorithm is, so if the value of unknown l is large, the data reconstruction performance of this time slot will not be guaranteed. To solve this problem, the unknown part of the equivalent channel matrix is reduced and the equivalent channel matrix is split, as shown in Eq. (13).

$$H_e^{(l)} = H_e^{(l-1)} + \Delta H_e^{(l)} . \tag{13}$$

In Eq. (13), $\Delta H_e^{(l)} = H^{(0)-1}\Delta H^{(i)}$, if the equivalent channel matrix $\Delta H_e^{(l)} = H^{(0)-1}\Delta H^{(i)}$ is known for the $l-1$ time slot, Eq. (14) can be obtained as follows.

$$\min\left\|x^{(l)}\right\|_1 \ s.t.\left\|y^{(l)} - \left(\hat{A}^{(l)} + E^{(l)}\right)x^{(l)}\right\|_2 < \varepsilon . \tag{14}$$

In Eq. (14), $\hat{A}^{(l)} = H_e^{(l-1)}A$ is the matrix that has been measured. $E^{(l)} = \Delta H_e^{(l)}A$ is the unknown perturbation matrix. In practice, the real rate of change of the channel is small, and the difference between the corresponding equivalent channels $H_e^{(l)}$ and $H_e^{(l-1)}$ between adjacent moments $\Delta H_e^{(l)}$ is also small. Therefore, the values of the elements in the unknown perturbation matrix $E^{(l)}$ are significantly lower than the values of the elements in the already measured matrix $\hat{A}^{(l)}$, which meets the conditions of the perturbation compression perception problem. In other words, the model can reconstruct the original data by using the perturbation compression-aware reconstruction algorithm. The reconstruction performance of the current time slot is only determined by the equivalent channel matrix of the previous time slot, which can effectively prevent the effect of the size of l value on the performance. Therefore, the equivalent channel of the previous time slot can be set as a unit matrix. But when the change rate of the channel is large, it will lead to a large total error value of $H_e^{(l)}$ for the equivalent channel of the l time slot, which finally greatly affects the reconstructed effect. In view of this, an update operation is implemented for the equivalent channel of each time slot, and a semi-blind channel estimation structure is introduced in the model, as shown in Eq. (15).

$$H_e^{(l)} = \left(diag\left(A\hat{x}^{(l)}\right)\right)^{-1} y^{(l)} . \tag{15}$$

Eq. (15) combines the least-squares estimation algorithm, and $\hat{x}^{(l)}$ is used to describe the reconstructed result of this time slot in Eq. (15). When the accuracy of $\hat{x}^{(l)}$ is high, it can ensure that the least squares channel estimation results also have high accuracy. The comparison of the channel estimation results obtained after optimization with the real channel is shown in Fig. 6.

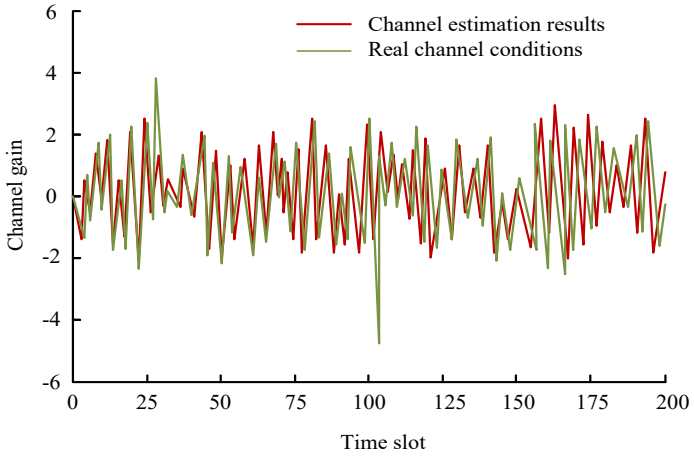

Fig. 6. Comparison of channel estimation results with real channel conditions

As can be seen in Fig. 6, the channel estimation results obtained after optimization are very close to the situation of the real channel. There is some noise and other perturbations in the process, so a few data with large deviations from the real channel appear. Combining the least-squares estimation algorithm to impose limits on the estimation results can limit the two estimates that are close to each other to a specified threshold without increasing the burden of the model operation. This threshold can remove the data broken by noise in the channel, allowing the whole model to operate properly. Meanwhile, the channel update part of the perturbed data transmission model ensures that the equivalent channel matrix works with low errors and that the perturbed compression-aware reconstruction algorithm can operate accurately. In addition, the high accuracy of the original data owned by the data reconstruction part also ensures that the channel estimation of the whole model has a better accuracy.

4 Performance Verification of Data Perturbation Compression-aware Reconstruction Algorithm and Improved Data Transmission Model

4.1 Performance Test of Data Perturbation Compression-aware Reconstruction Algorithm

To verify the performance of improved data perturbation compression-aware reconstruction algorithm for compressing and reconstructing wireless communication data with perturbations, the simulation test is carried out, in which the wireless communication block information with sparsity K, length $N = 500$ and block length $L = 5$ is selected as the simulation test data. The positions of non-zero elements in the data are generated by random generation, and their magnitude values satisfy the standard state distribution. The size of A is specified as $M \times N$ and all elements in A are set to satisfy the independent Gaussian distribution $X \sim N(0,1/\sqrt{M})$. The elements of the additive noise w and the perturbation matrix E are also generated from independent Gaussian distribution data and satisfy $\varepsilon_w = \|w\|_2 / \|A\|_2$ and $\varepsilon_E = \|E\|_2 / \|A\|_2$ respectively. ε_E and ε are the quantized values of the additive noise and the measurement matrix L respectively. The mean square error MSE is used as the performance evaluation index of the algorithm, and the unimproved classical BOMP algorithm is the comparison algorithm. All experimental schemes need to be repeated 20 times to take the average value as the final calculation result so as to improve the reliability of the simulation experimental results. After completing this simulation test, the performance of PBOMP algorithm and BOMP algorithm under different noise intensity is firstly counted, which is shown in Fig. 7.

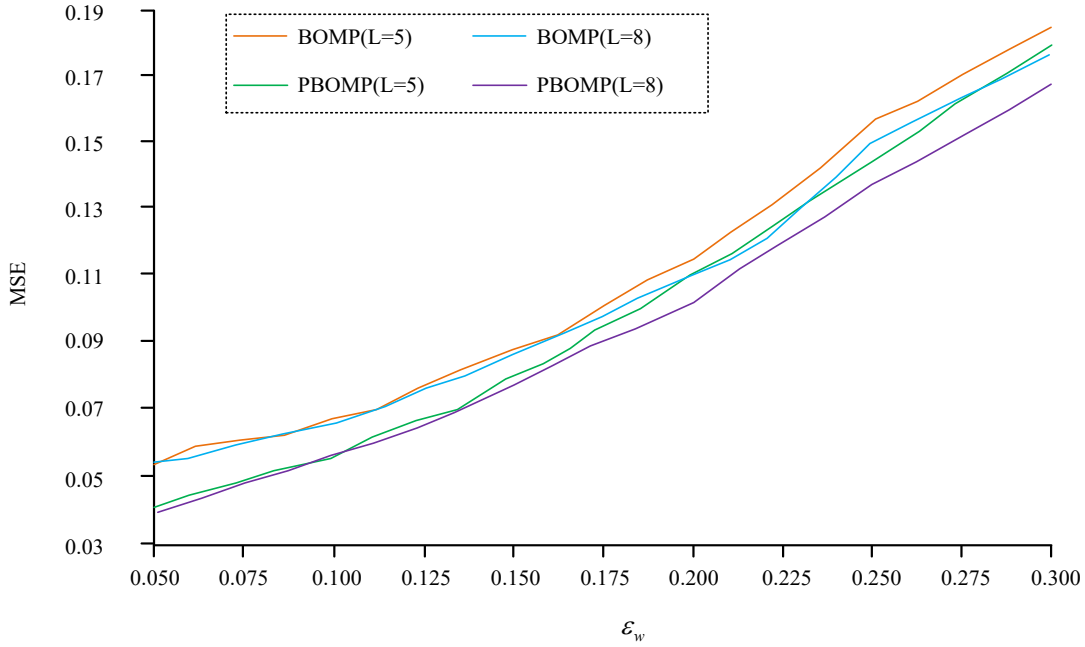

Fig. 7. Performance comparison of two perturbation compression-aware reconstruction algorithms under different noise intensities

Four experimental parameter schemes exist in Fig. 7, which they are PBOMP algorithm, BOMP algorithm and two choices of two metrics with a block length of 5 or 8 for the simulation test data. Observing Fig. 7, the MSE values obtained from each experimental scheme processing the simulation test data show a monotonically increasing trend as the value of ε_w grows. From the perspective of the perturbation compression-aware algorithm, the MSE values of the PBOMP algorithm designed in this study are significantly lower than those of the BOMP algorithm under the same data block length condition. Specifically, when the data block length is 5 and ε_w = 0.300, the computed MSE of PBOMP algorithm and BOMP algorithm are 0.179 and 0.186 respectively. The MSE of PBOMP algorithm is 0.007 lower than that of BOMP algorithm. When the data block length is 8 and ε_w = 0.300, the computed MSE of PBOMP algorithm and BOMP algorithm are 0.167 and 0.176 respectively. The MSE of PBOMP algorithm is 0.009 lower than that of BOMP algorithm. It indicates that the anti-disturbance performance of PBOMP algorithm designed in this study is better than that of traditional BOMP algorithm. Then the performance of PBOMP algorithm and BOMP algorithm under different sparsity is analyzed, which is shown in Fig. 8.

The horizontal axis in Fig. 8 represents the sparsity, and its value range is set from 2 to 12 according to the common values in wireless network data. The vertical axis still represents the MSE, and different colors show different experimental schemes. Analyzing Fig. 8, the MSE values obtained from each experimental scheme processing the simulation test data also demonstrate a monotonically increasing trend as the sparsity increases. From the perspective of the perturbation compression-aware algorithm, the MSE values of the PBOMP algorithm designed in this study are significantly lower than those of the BOMP algorithm under the same ε_E conditions. Specifically, when the sparsity is 6 and ε_E = 0.05, the computed MSE of PBOMP algorithm and BOMP algorithm are 0.02 and 0.03 respectively. The MSE value of PBOMP algorithm is 0.01 lower than that of BOMP algorithm. When the sparsity is 6 and ε_E = 0.15, the computed MSE of PBOMP algorithm and BOMP algorithm are 0.07 and 0.22 respectively. The MSE value of PBOMP algorithm is 0.15 lower than that of BOMP algorithm. When the sparsity is 12 and ε_E = 0.05, the MSE of PBOMP algorithm and BOMP algorithm is 0.04 and 0.06 respectively. The MSE value of PBOMP algorithm is 0.02 lower than that of BOMP algorithm. When the sparsity is 12 and ε_E = 0.15. The MSE of PBOMP algorithm and BOMP algorithm is 0.12 and 0.29 respectively. The MSE value of PBOMP algorithm is 0.17 lower than that of BOMP algorithm. It indicates that the anti-disturbance performance of PBOMP algorithm designed in this study is better than that of traditional BOMP under all sparsity conditions algorithm. Fig. 8 also shows that the MSE growth of PBOMP algorithm is significantly smaller than that of

BOMP algorithm with the growth of sparsity, which means that the former is more adaptable to sparsity and has better algorithm robustness.

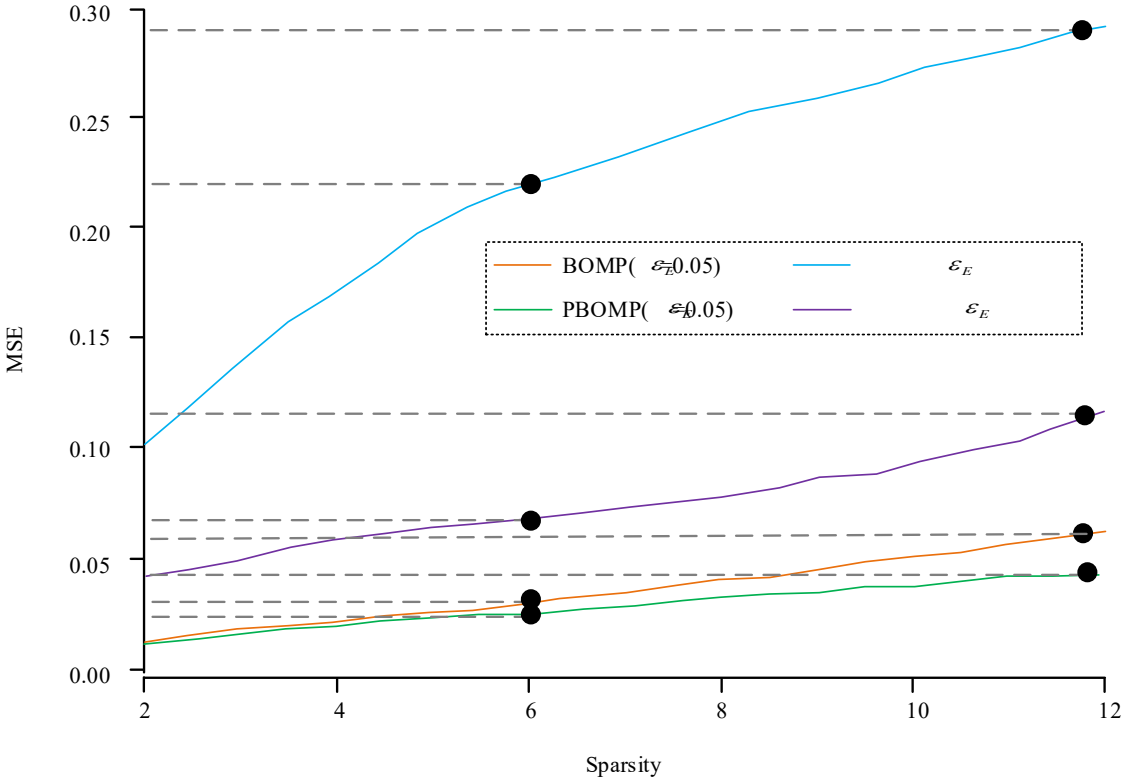

Fig. 8. Performance comparison of two perturbation compression-aware reconstruction algorithms with different noise sparsity

4.2 Improved Wireless Data Transmission Model Performance Verification

To verify the performance of the wireless network data transmission model constructed based on the PBOMP algorithm, a series of simulation experiments are designed again. There are three experimental schemes. The first one is the wireless network data transmission model based on the PBOMP algorithm proposed in this study (later referred to as PBOMP Model). The second one is the conventional scheme based on the BOMP algorithm to build the model (later referred to as BOMP Model). The third one is the perfect channel scheme (later referred to as H_BOMP Model). The characteristics of the three schemes are as follows: the receiver performs channel estimation at time slot 0 and then alternates between data reconstruction and channel update; the receiver performs channel estimation at time slot 0 and uses the estimation result to reconstruct the information of the whole frame; there is no any real channel influence. The experimental simulation results are the average values of 2000 frames transmitted by each experimental scheme, and each frame is composed of L data time slots and 1 pilot frequency time slot. According to the real operating environment of wireless communication network, the basic parameters of the data to be transmitted in this simulation experiment are set as block length B and length N of 4 and 400 respectively. Gaussian white noise is artificially mixed in each frame, and its variance is σ^2. The measurement matrix is a random matrix, generated by a standard normal distribution. Each transmission model sends the compressed data of length M to the receiver using time-varying channel, and the receiver will try to reconstruct the original communication data without identifying the signal sparsity. The performance evaluation index of the scheme is MSE. After the simulation experiments are completed, the performance of the three data transmission models under different noise intensities is calculated and shown in Fig. 9.

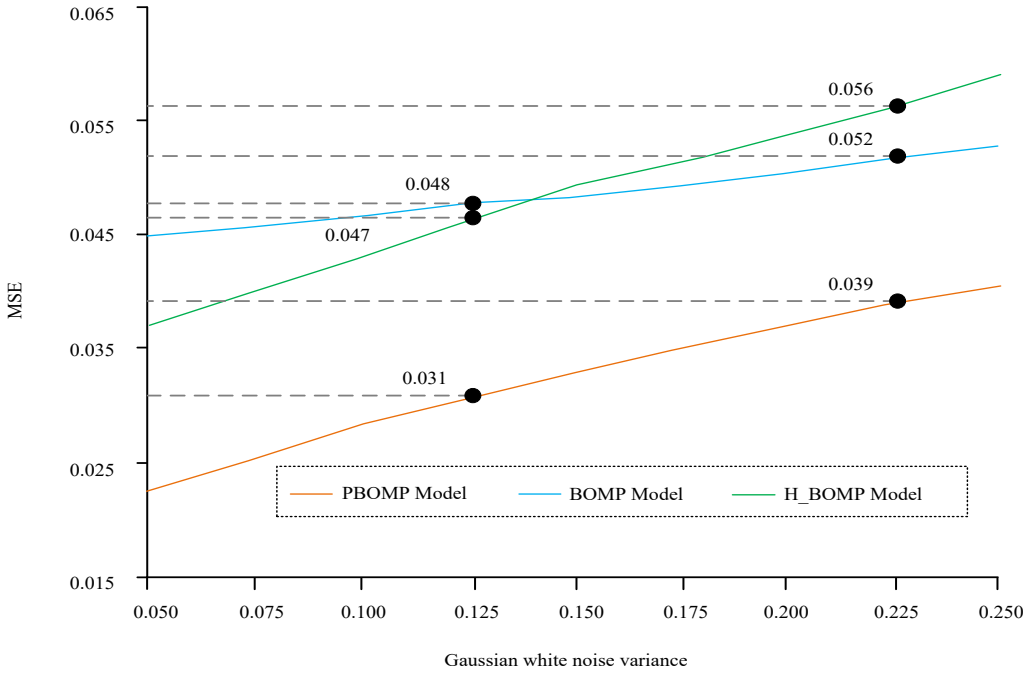

Fig. 9. Performance comparison of three wireless network signal transmission schemes at different noise strengths

The horizontal axis in Fig. 9 shows the variance of Gaussian white noise, which is used to evaluate the information noise intensity. Different colors represent different data transmission model schemes, and the gray dashed line is used to assist in showing the MSE value corresponding to a certain point. Observing Figure 9, the MSE values of each transmission scheme show an overall increasing trend as the information white noise intensity increases, but the MSE values of the PBOMP Model scheme proposed in this study are the smallest under any same noise intensity condition. For example, when the variance of Gaussian white noise is 0.125, PBOMP model, BOMP model and H_ MSE of BOMP model are 0.031, 0.048 and 0.047 respectively; the MSE of the PBOMP model is 0.017 and 0.016 lower than that of the other two models. When the variance of Gaussian white noise is 0.225, PBOMP model, BOMP model and H_ MSE of BOMP model are 0.039, 0.052 and 0.056 respectively; the MSE of the PBOMP model is 0.013 and 0.017 lower than that of the other two models. Finally, the performance of each data transmission scheme under different compressed data lengths is analyzed, as shown in Fig. 10.

Observing Fig. 10, the MSE of each wireless network signal transmission model shows an overall decreasing trend as the compressed data length increases. However, the PBOMP Model proposed in this study has the smallest MSE value for the same compressed data length. For example, when the compressed data length is 210, PBOMP model, BOMP model and H_ MSE of BOMP model are 0.028, 0.047 and 0.042 respectively; the PBOMP model proposed in the study are 0.019 and 0.014 lower than the other two models respectively. When the compressed data length is 250, PBOMP model, BOMP model and H_ MSE of BOMP model are 0.024, 0.044 and 0.039 respectively; the proposed PBOMP model is 0.02 and 0.015 lower than the other two models respectively. Through the above analysis, compared with the traditional classical model and the perfect transmission model, this method has a good effect under different noise intensity and different compressed data length. The model proposed in this paper uses the reconstruction algorithm in the compressed sensing theory to solve the interference problem of noise and other factors in the data transmission process. On the basis of traditional methods, the error rate of channel matrix is reduced, and the accuracy of data transmission model is improved.

In conclusion, the MSE value of the proposed algorithm based on perturbation compression sensing is lower than that of the other two methods under different block lengths and different sparsity conditions. At the same time, under different information white noise intensity and data length, the proposed signal transmission models have lower MSE values. Therefore, the wireless network communication signal reconstruction method based on perturbation compressed sensing has better performance and transmission effect, and can effectively meet the quality requirements of signal transmission.

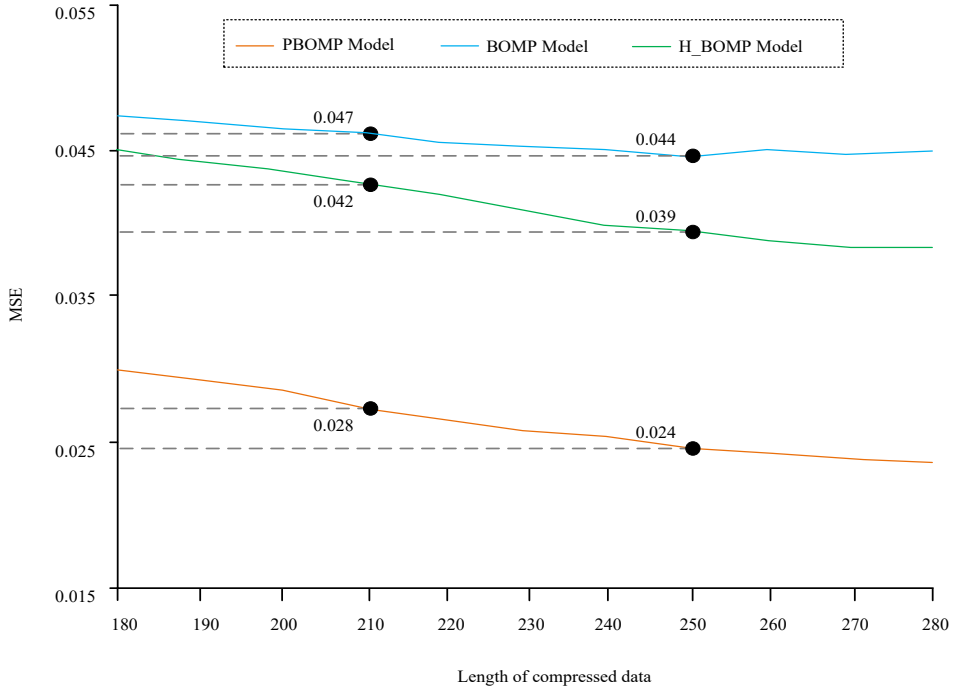

Fig. 10. Performance comparison of three wireless network signal transmission schemes with different compressed data lengths

5 Conclusion

In this study, an improved perturbation-compression-aware reconstruction algorithm that can be used to process block-structured data is designed to solve the block sparse structure of wireless network communication data. A single-user wireless network communication data transmission model is constructed based on this algorithm. Through experiments, the following research results are obtained. The MSE values of the improved perturbation-compression-aware reconstruction algorithm are significantly lower than those of the traditional BOMP algorithm under different noise intensities and different noise sparsity. The MSE values of the data transmission model constructed based on this improved algorithm are also lower than those of the classical transmission model and the perfect transmission model under different noise intensities and different compressed data lengths. Specifically, when the variance of Gaussian white noise is 0.125, the MSE values of PBOMP model, BOMP model and H_BOMP model are 0.031, 0.048 and 0.047 respectively. When the compressed data length is 210, the MSE values of the three models are 0.028, 0.047 and 0.042 respectively. The experimental data prove that the improved perturbation-aware reconstruction algorithm based on wireless network communication data transmission model designed in this study can effectively reduce the influence of perturbation in the signal and improve the robustness of data transmission model. This research result can provide some reference and support for improving the quality of data transmission. However, the reconstruction algorithm has always been one of the key and difficult points in the field of compression sensing theory, and there are many optimization methods for the reconstruction algorithm. Therefore, in the subsequent research, it is necessary to consider the impact of more processing methods of reconstruction algorithms on the quality of data transmission, so as to further improve the quality of data transmission.

Acknowledgements

The research is supported by 2022 Nanjing Vocational College of Information Technology school-level Fund

“Research on interference suppression and signal reconstruction in wireless” (YK20220502).

References

[1] Z. Hu, Y. Wang, M.F. Ge, J. Liu, Data-driven fault diagnosis method based on compressed sensing and improved multi-scale network, IEEE Transactions on Industrial Electronics 67(4)(2020) 3216-3225.
[2] B. Yan, L. Jian, R. Ren, J. Fulk, E. Sidnam-Mauch, P. Monge, The paradox of interaction: communication network centralization, shared task experience, and the wisdom of crowds in online crowdsourcing communities, Communication Research 48(6)(2021) 796-818.
[3] M.S. Shamim, R.S. Narde, J.L. Gonzalez-Hernandez, A. Ganguly, J. Venkatarman, S.G. Kandlikar, Evaluation of wireless network-on-chip architectures with microchannel-based cooling in 3D multicore chips, Sustainable Computing, Informatics and Systems 21(2019) 165-178.
[4] M. Sun, J. Zhou, B. Dong, Y. Le, S. Zheng, Disturbance force self-sensing and suppression method for AMB-rotor system based on disturbance observer, IEEE Sensors Journal 20(16)(2020) 9245-9252.
[5] J. Linke, G.J. McDermid, A.D. Pape, A.J. McLane, D.N. Laskin, M. Hall-Beyer, S.E. Franklin, The influence of patch-delineation mismatches on multi-temporal landscape pattern analysis, Landscape Ecology 24(2)(2009) 157-170.
[6] S. Cao, C. Dai, Y. Zhu, W. Chen, A novel compressed sensing-based recognition method for power quality disturbance signals, Dianli Xitong Baohu yu Kongzhi/Power System Protection and Control 45(3)(2017) 7-12.
[7] J. Wang, Z. Xu, Y. Che, Power quality disturbance classification based on compressed sensing and deep convolution neural networks, IEEE Access 7(2019) 78336-78346.
[8] Y. Liu, W. Tang, Incoherence analysis of RD-AIC-based observation matrix and its application in power quality disturbance signal, Mathematical Problems in Engineering 2021(2021) 1-12.
[9] S.A. Saeed, F.Z. Khan, Z. Iqbal, R. Alroobaea, M. Ahmad, M. Talha, M.A. Raza, A. Ihsan, An IoT-based network for smart urbanization, Wireless Communications and Mobile Computing 2021(2021) 1-14.
[10] C. Jiang, Retracted: Network security and ideological security based on wireless communication and big data analysis, Wireless Communications and Mobile Computing 2022(2022) 1-6.
[11] W. Shi, Y. Liu, Z. Peng, M. Xu, Z. Zhang, The design of deploying RIS for millimetre-wave signal in outdoor environment, Wireless Communications and Mobile Computing 2021(2021) 1-6.
[12] Y. Wang, Q. Lu, Y. Jin, H. Zhang, Communication modulation signal recognition based on the deep multi-hop neural network, Journal of the Franklin Institute 358(12)(2021) 6368-6384.
[13] D. Naman, M. Abdulwahab, A. Ibrahim, RADIUS authentication on unifi enterprise system controller using zero-handoff roaming in wireless communication, Journal of Applied Science and Technology Trends 1(3)(2020) 118-124.
[14] M. Huang, S. Liu, Z. Li, S. Feng, D. Wu, Y. Wu, F. Shu, Remote sensing image fusion algorithm based on two-stream fusion network and residual channel attention mechanism, Wireless Communications and Mobile Computing 2022(2022) 1-14.
[15] S. Zhang, Link loss inference algorithm with network topology aware in communication networks, Mathematical Problems in Engineering 2020(2020) 1-10.
[16] C. Seguin, T. Ye, A. Zalesky, Network communication models improve the behavioral and functional predictive utility of the human structural connectome, Network Neuroscience 4(4)(2020) 1-40.
[17] F. Semmelmann, K. Straub, J. Nazet, C. Rajendran, R. Merkl, R. Sterner, Mapping the allosteric communication network of aminodeoxychorismate synthase, Journal of Molecular Biology 431(15)(2019) 2718-2728.
[18] C. Cheng, Y. Jiang, Q. Sun, Spatially distributed sampling and reconstruction, Applied and Computational Harmonic Analysis 47(1)(2019) 109-148.
[19] N. Gupta, P.M. Pawar, S. Jain, Improve performance of wireless sensor network clustering using mobile relay, Wireless Personal Communications 110(2)(2020) 983-998.
[20] H. Qiang, Consumption reduction solution of TV news broadcast system based on wireless communication network, Complexity 2021(2021) 1-13.